TECHNOMETRICS, MAY 1989, VOL. 31, NO. 2

Graphical Assessment of the Prediction Capability of Response Surface Designs

Ann Giovannitti-Jensen and Raymond H. Myers

Department of Statistics
Virginia Polytechnic Institute
and State University
Blacksburg VA 24061

Measures of the quality of prediction at locations on the surface of a hypersphere are presented. These measures are used to form a graphical method of assessing the overall prediction capability of an experimental design throughout the region of interest. A plot of the spherical variance and the maximum and minimum prediction variances for locations on a sphere against the radius of the sphere, a *variance dispersion graph*, is used to give a comprehensive picture of the behavior of the prediction variances throughout a region and hence of the quality of the predicted responses obtained with a particular design. Such plots are used to investigate and compare the prediction capabilities of certain response surface designs currently available to the researcher.

KEY WORDS: Dispersion graphs; Efficiency; Prediction variance; Spherical measures.

1. THE RESPONSE SURFACE DESIGN PROBLEM

Since the landmark article by Box and Wilson (1951), researchers have proposed many criteria for evaluating and comparing response surface designs. Response surface methodology (RSM) often involves the fitting by the method of least squares of a first-order regression model

$$y = b_0 + \sum_{i=1}^{k} b_i x_i + \varepsilon \qquad (1.1)$$

or a second-order model

$$y = b_0 + \sum_{i=1}^{k} b_i x_i + \sum_{i=1}^{k} b_{ii} x_i^2 + \sum\sum_{i<j} b_{ij} x_i x_j + \varepsilon \qquad (1.2)$$

to a set of data in which $x_1, x_2, \ldots, x_k$ represent a set of design variables, y represents a measured response, and ε is a random error with mean 0 and variance σ^2. The properties of these response surface models are dictated by theory of the general linear model $\mathbf{y} = X\boldsymbol{\beta} + \boldsymbol{\epsilon}$, where X is the model matrix, influenced by the experimental design and the random vector $\boldsymbol{\epsilon}$ is assumed to have mean $\mathbf{0}$ and dispersion matrix $\sigma^2 I$. Box and Wilson (1951) introduced the notion of composite designs in which a two-level factorial or fractional factorial design is augmented by "star" points that allow for estimation of pure quadratic terms in the fitted model of Equation (1.2). Other response surface designs to rival the composite designs were proposed by Box and Behnken (1960). Illustrations of the use of such response surface designs appear in works by Box and Draper (1987), Khuri and Cornell (1987), and Myers (1976). Design classes motivated by Kiefer's (1959) design-optimality criteria were proposed in the 1970s and 1980s (see Box and Draper 1971, 1974; Hoke 1974; Mitchell and Bayne 1978; Notz 1982). The easy access to experimental plans that are *D-efficient* is the prime motivation for the development of many of these designs. D-efficiency is based on the maximization of the determinant of $X'X$ (see, e.g., Atwood 1969). D-efficient designs result in relatively small values of the generalized variance of the coefficients. The practical value of D-optimality was reviewed by St. John and Draper (1975).

Single Number Design Criteria

Attempts to compare response surface designs have been made on the basis of single-valued efficiency-type criteria. There is an abundance of literature on D-efficiency in connection with response surface designs. Among these are works by Lucas (1974, 1976), Nalimov, Golikova, and Mikeshina (1970), and many others. The concept of D-efficiency suggests a simple and interesting *single number criterion* for design construction and for comparing designs. D-efficiency obviously accommodates the notion of estimation of regression coefficients. The success of a response surface study is best quantified,

however, through the consideration of the prediction variance function

$$\frac{N(\text{var } \hat{y}(\mathbf{x}))}{\sigma^2} = N\mathbf{f}'(\mathbf{x})(X'X)^{-1}\mathbf{f}(\mathbf{x}), \quad (1.3)$$

where the vector-valued function $\mathbf{f}(\mathbf{x})$ represents an arbitrary point in the model space and contains the model terms characterized by the rows of the X matrix. The matrix $(X'X)^{-1}$ is the variance–covariance matrix of the regression coefficients (apart from σ^2). It is difficult to accurately characterize the performance of N var $\hat{y}(\mathbf{x})/\sigma^2$ with a single number. Box and Draper (1959, 1963) used the notion of the average variance or integrated prediction variance

$$\text{IV} = N\frac{K}{\sigma^2}\int_R \text{var } \hat{y}(\mathbf{x})\, d\mathbf{x}$$

over a region of interest R to develop designs that are robust against model misspecification. Here K is the inverse of the volume of the region R. The criterion, however, does not address the notion of general behavior and stability of N var $\hat{y}(\mathbf{x})/\sigma^2$ throughout the experimental design region or the region in which the user desires good prediction or estimation of response. Many RSM designs experience a deterioration of N var $\hat{y}(\mathbf{x})/\sigma^2$ on or near the design perimeter. It is often important for the experimenter to estimate the response well near the design perimeter. On the other hand, some designs may experience "weak spots" in the design interior even though the "average" prediction variance is reasonably good.

The criterion of G-efficiency certainly is attentive to the performance of the variance function. The G-optimal design minimizes the maximum value (over the design region) of N var $\hat{y}(\mathbf{x})/\sigma^2$. Lucas (1976) considered G-efficiency in the comparison of response surface designs. G-efficiency is calculated for a specific design as $p/(\max N \text{ var } \hat{y}(\mathbf{x})/\sigma^2)$, where p is the number of model parameters and the maximization is taken over all $\mathbf{x}$ in the design region. A G-optimal design has max N var $\hat{y}(\mathbf{x})/\sigma^2 = p$. G-efficiency is certainly an important measure but, as a single number criterion, it does not supply sufficient information regarding the behavior of the variance function.

The choice of RSM design parameters with the intent of stabilizing prediction variance was considered by Box and Hunter (1957). They developed the notion of a rotatable design that guarantees equality of N var $\hat{y}(\mathbf{x})/\sigma^2$ on spheres with origins at the design center. At the time, they used the number of center runs of the design to exert some control over the *distribution* of N var $\hat{y}(\mathbf{x})/\sigma^2$ from the design center to the design perimeter. Their purpose was to gain stability beyond what is provided by rotatability. Draper (1982) shed more light on center runs and stability of prediction variance for a rotatable design.

For any response surface design, there are locations in the design region where responses are estimated well and locations where estimation is relatively poor. The concept of a design in which the variance function is constant everywhere in the design space represents wishful thinking. The user deserves to have a total assessment of prediction capability and stability. This total picture is often not supplied by a scalar numerical criterion.

2. GRAPHICAL METHODS TO EVALUATE DESIGNS

In recent years, more statisticians have recognized the value of graphical methods in data analysis. Since the performance of an experimental design (particularly in an RSM setting) so obviously presents a multidimensional problem, it would seem that creative graphical techniques in comparing and evaluating designs would be an obvious approach. In the following subsections, we provide the building blocks for a "variance footprint" of an arbitrary RSM design through a single two-dimensional picture.

2.1 Assessment of Prediction Capability on Spheres

In a general RSM setting, the variance of a predicted response at a given location is a function of more than merely the distance of the location from the design center. We can begin our development by considering the spherical average prediction variance or *spherical variance*, V^r, the average of the variances of the estimated responses *over the surface of a sphere*, a quantity given by

$$V^r = N\frac{\Psi}{\sigma^2}\int_{U_r} \text{var}(\hat{y}(\mathbf{x}))\, d\mathbf{x}, \quad (2.1)$$

where $U_r = \{\mathbf{x} : \sum_{i=1}^k x_i^2 = r^2\}$ and $\Psi^{-1} = \int_{U_r} d\mathbf{x}$ is the surface area of U_r. The spherical variance was used by Hussey, Myers, and Houck (1987) in evaluating RSM designs for simulation models. By the definition of $\mathbf{f}(\mathbf{x})$ in Equation (1.3), we can write the response surface model for a single y as $E(y) = \mathbf{f}'(\mathbf{x})\boldsymbol{\beta}$. Hussey et al. (1987) showed that the spherical variance V^r is written as

$$V^r = \text{tr } S(X'X)^{-1}, \quad (2.2)$$

where S is the matrix of *region moments*, the region being the hypersphere defined by U_r. S can be written

as

$$S = \Psi \int_{U_r} \mathbf{f}(\mathbf{x})\mathbf{f}'(\mathbf{x})\, d\mathbf{x}. \qquad (2.3)$$

The concept of region moments is the same as that used by Box and Draper (1959, 1963) and Draper and Lawrence (1965), the exception being that U_r is the surface of a hypersphere. The relevant region moments that are dependent on the model being used are functions of the radius r and k, the dimension of the hypersphere. For example, if the model is first order, the relevant region moments for computing V^r are moments through order 2. Details of the integration over the hypersphere were given by Stroud (1971). Spherical moments through order 4 appear in Appendix A. Illustrations of the form of the S matrix for first-order and second-order models are given.

To illustrate the use of the spherical variance, consider two first-order designs, D_1, a 2^3 factorial, and D_2, a 2^3 factorial with the points $[-1, -1, -1]$ and $[+1, +1, +1]$ missing. Figure 1 provides a plot of V^r against r for both designs to illustrate the impact of the two missing observations from the orthogonal design. Notice that V^r, the *average variance on a sphere* for the two designs, is quite similar until we consider regions close to the design perimeter. The superiority of the orthogonal design becomes apparent at roughly a distance $r = 1.0$ from the design center. The superiority is more pronounced at the design perimeter, $r = \sqrt{3}$.

It is predictable that the 2^3 factorial should be superior to the nonorthogonal six-point design. A plot

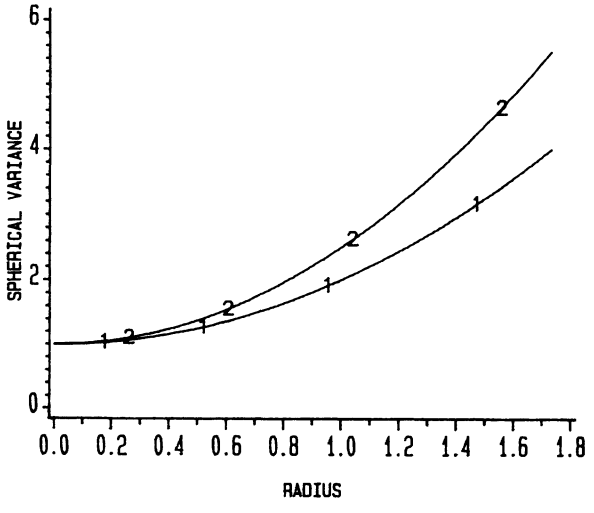

Figure 1. Comparison of Spherical Variances for Two First-Order Designs. Design 1 is a 2^3 factorial design with no center runs, N = 8; design 2 is a 2^3 factorial with two missing runs and no center runs, N = 6. Variances are weighted by sample size.

of the two spherical variances is helpful, but additional information is needed to gain more insight into the behavior of the variance function for competing designs. In this case, the plot is an accurate depiction of the stability of the variance function for the orthogonal 2^3 plan since, as a rotatable design, N var $\hat{y}(\mathbf{x})/\sigma^2$ is constant on spheres. But in the case of the six-point design, it does not give the true picture of how much variability in the variance function exists around V^r, the average value of N var $\hat{y}(\mathbf{x})/\sigma^2$ on spheres. The material in the following sections outlines methods of depicting dispersion around V^r.

2.2 Use of Prediction Variance Dispersion Measures

It is important to supplement the plot of V^r of Equation (2.2) with some measure that depicts the lack of stability of the variance function as a deviation from the "average" given by V^r. One needs to capture in a graphical way a sense of the *distribution* of N var $\hat{y}(\mathbf{x})$ as a function of r. Two such measures are the *range* and the "standard deviation." We define the range of N var $\hat{y}(\mathbf{x})/\sigma^2$ on a sphere of radius r as

$$R \text{ of } V(r) = \max_{\mathbf{x}\in U_r} \left[\frac{N \text{ var } \hat{y}(\mathbf{x})}{\sigma^2}\right] - \min_{\mathbf{x}\in U_r} \left[\frac{N \text{ var } \hat{y}(\mathbf{x})}{\sigma^2}\right],$$

and the "standard deviation" as the square root of

$$V \text{ of } V(r) = \Psi \int_{U_r} \left[\frac{N \text{ var } \hat{y}(\mathbf{x})}{\sigma^2} - V^r\right]^2 d\mathbf{x}.$$

(We do not pursue the "standard deviation" dispersion measure with illustrations because of the obvious difficulty in interpretation.) Fairly simple expressions for the dispersion measures can be developed for the case of a first-order model. For the case of a second-order RSM model, one has access to these measures using readily available computing algorithms.

2.3 Dispersion Measures for the First-Order Model

In the case of the first-order model in Equation (1.1), it is necessary to consider two specific cases. Consider first the situation that exists for many standard first-order designs. The location of the design origin, centered to the levels $(0, 0, \ldots, 0)$, is the same as the center of the *region of interest*, the latter being defined as the center of spheres on which the variance function is being computed. We refer to this situation as case 1. For certain nonstandard or ill-

designed plans (missing data points, etc.), these two centers may not be the same. This will be referred to as case 2. Under case 1, V^r and the two dispersion measures are simple functions of the eigenvalues of $(X'X)^{-1}$ and the radius at which the dispersion measure is being evaluated.

If we apply the general form of V^r in Equation (2.2) and make use of the region moment $\sigma_2 = r^2/k$ (from App. A), we obtain

$$V^r = 1 + \frac{Nr^2}{k} \sum_{i=1}^{k} \lambda_i, \tag{2.4}$$

where the λ_i are the eigenvalues of $(X'X)^{-1}$. Equation (2.4) indicates that in this case 1 situation, the average prediction variance on a sphere of radius r is a simple function of the average of the eigenvalues of $(X'X)^{-1}$ and r^2. The details are supplied in Appendix B.

The extremes of N var $\hat{y}(\mathbf{x})/\sigma^2$ on a radius r and hence R of $V(r)$ are simple to compute for case 1. In fact,

$$\max_{\mathbf{x} \in U_r} \frac{N \text{ var } \hat{y}(\mathbf{x})}{\sigma^2} = 1 + N(\lambda_{\max})r^2 \tag{2.5}$$

and

$$\min_{\mathbf{x} \in U_r} \frac{N \text{ var } \hat{y}(\mathbf{x})}{\sigma^2} = 1 + N(\lambda_{\min})r^2. \tag{2.6}$$

As a result,

$$R \text{ of } V(r) = N(\lambda_{\max} - \lambda_{\min})r^2. \tag{2.7}$$

Here, $\lambda_{\max}$ and $\lambda_{\min}$ are, respectively, the largest and smallest eigenvalues of $(X'X)^{-1}$ (see App. B). The expression for V of $V(r)$ is also quite simple. It turns out that

$$V \text{ of } V(r) = \frac{N2r^4}{k(k+2)} \sum_{i=1}^{k} (\lambda_i - \bar{\lambda})^2. \tag{2.8}$$

The proof of the result for R of $V(r)$ appears in Appendix B. It turns out then, as expected, that if all of the eigenvalues are equal, both measures are 0, a characteristic of an orthogonal and thus rotatable first-order design. In cases in which eigenvalues are not distinct, maximum and minimum values of N var $\hat{y}(\mathbf{x})/\sigma^2$ on U_r may occur at more than one location.

It is interesting but not unexpected that for designs that are not "messy" (case 1) the dispersion in N var $\hat{y}(\mathbf{x})/\sigma^2$ on a sphere is proportional to the corresponding dispersion in the eigenvalues. These simple relationships allow us to establish properties of both the V^r and the dispersion measures, some of which also hold for designs that do not fall into case 1. In what follows, we will use R of $V(r)$ as the dispersion measure depicted graphically because of its simplicity in interpretation for the user.

Suppose we return to the earlier illustration with the 2^3 factorial and the nonorthogonal six-point design. Figure 2 shows on the same picture the *variance dispersion graphs* (VDG's) for the two designs. These graphs are similar in structure to the ridge plots of Hoerl (1959) in which maximum response on a sphere is plotted against radius. The 2^3 design has a dispersion of 0. Thus its total variance picture is characterized by the V^r plot. The difficulty with the nonorthogonal six-point design is now characterized. The maximum and minimum values of N var $\hat{y}(\mathbf{x})/\sigma^2$ depict an uncomfortable instability of prediction variance around V^r as one proceeds toward the design perimeter.

We have indicated on the graph, for reference, parameter lines at $p = 4$ and $2p = 8$. This gives the viewer a clear indication of the G-efficiency of the designs being studied. The 2^3, of course, achieves 100% G-efficiency with N var $\hat{y}(\mathbf{x})/\sigma^2 = p$ at the design perimeter, whereas the G-efficiency of the six-point design is below 50% depicted by the $2p = 8$ line. Hereafter, all VDG's illustrated will have the p and $2p$ lines displayed.

The illustrations shown here are, of course, case 1 designs. Analytic expressions for V^r, R of $V(r)$, and V of $V(r)$ for case 2 are not particularly appealing and hence we will not display them here. Results and details for V^r and R of $V(r)$ appear in Appendix B. Computation of R of $V(r)$ can be accomplished with an optimization algorithm. Further discussion of such an algorithm appears in Section 3.

2.4 Graphical Illustration of the Effect of Design Augmentation

Consider the following irregular first-order design ($N = 17$) for fitting a first-order model with four

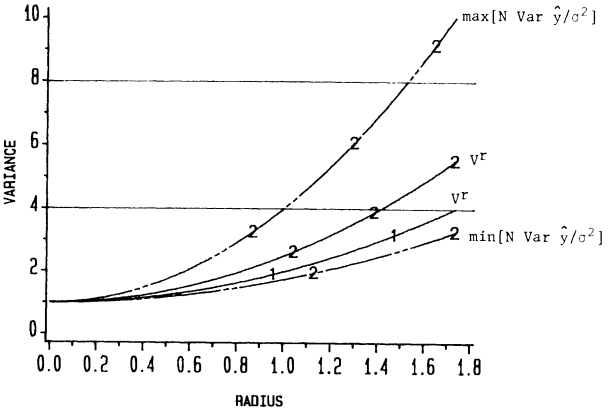

Figure 2. Variance Dispersion Graphs for Two First-Order Designs. Design 1 is a 2^3 factorial design with no center runs, $N = 8$; design 2 is a 2^3 factorial with two missing runs and no center runs, $N = 6$. Variances are weighted by sample size.

design variables:

$$D = \begin{array}{c} \begin{matrix} x_1 & x_2 & x_3 & x_4 \end{matrix} \\ \begin{bmatrix} 1 & 1 & 1 & 1 \\ 1 & 1 & 1 & -1 \\ 1 & 1 & 1 & 1 \\ -1 & -1 & -1 & 1 \\ 1 & 1 & 1 & 1 \\ 1 & 1 & -1 & -1 \\ 1 & -1 & 1 & -1 \\ 1 & 1 & 1 & -1 \\ -1 & -1 & -1 & 1 \\ -1 & -1 & -1 & 1 \\ -1 & -1 & 1 & 1 \\ 1 & 1 & -1 & -1 \\ -1 & -1 & 1 & -1 \\ -1 & 1 & -1 & -1 \\ -1 & -1 & -1 & 1 \\ -1 & -1 & -1 & -1 \\ 0 & 0 & 0 & 0 \end{bmatrix} \end{array} \qquad (2.9)$$

Figure 3 gives the variance dispersion graph depicting the average prediction variance and the maximum and minimum prediction variance as a function of r. The design is not orthogonal and it is clear from the picture that a severe loss of efficiency is experienced when one uses this design for predicting the response. The VDG for a 2^4 design with one center run is shown on the same graph. It is of interest to determine the locations of the maximum variance as a function of r. Figure 4 shows the locations in the four design variables. The figure indicates that the point at which N var $\hat{y}(\mathbf{x})/\sigma^2$ is maximum in, say, a *spherical region of interest of radius 2 from the design center* is given by $x_1 = 1.50$, $x_2 = -1.20$, $x_3 = -.561$, and $x_4 = .094$. Suppose that we wish to study

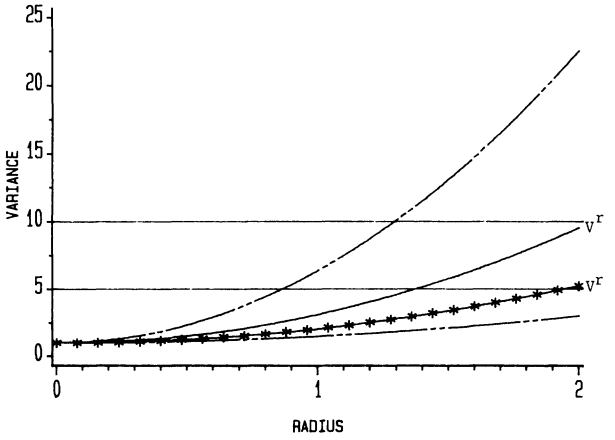

Figure 3. Variance Dispersion Graph for the Two-Level First-Order Design Given by Equation (2.9). Spherical variances for a 2^4 are denoted by --. Variances are weighted by sample size (N = 17).*

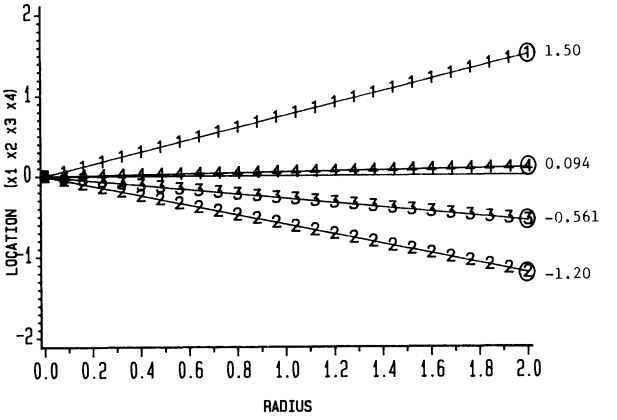

Figure 4. Locations of Maximum Prediction Variance on Spheres for the Two-Level First-Order Design Given by Equation (2.9). For a location on a given sphere of radius r, 1 denotes the value of the variable x_1, 2 denotes the value of the variable x_2, 3 denotes the value of the variable x_3, and 4 denotes the value of the variable x_4.

the effect of an augmentation of the design, in which an additional point is taken at these coordinates. Figure 5 illustrates the increase in efficiency for the augmented design. Please note that as in all other cases the prediction variance is weighted by sample size.

The plot of the VDG for the augmented design shows only a moderate decrease in the average variance V^r but a dramatic improvement in the maximum prediction variance throughout most of the design region. There is a 45% reduction in the maximum prediction variance at the design perimeter. The example illustrates a graphical look at gain provided by augmenting an RSM design through an augmentation procedure such as DETMAX (Mitchell 1974). The point chosen is that which most enhances the variance–covariance properties of the coefficients—

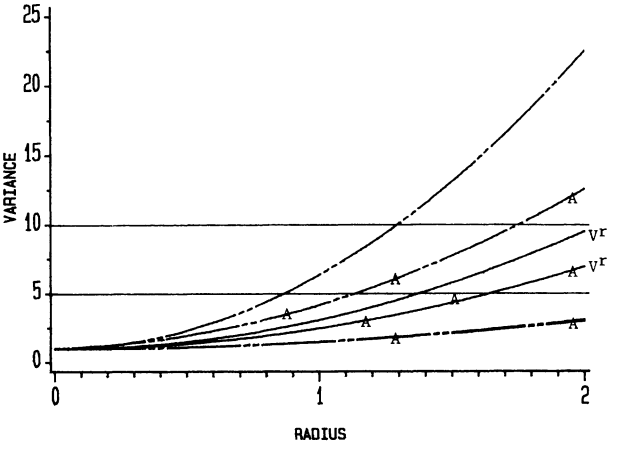

Figure 5. Variance Dispersion Graphs for the Two-Level First-Order Design and for the Same Design With a Design Point Augmented. Variances for the augmented design are represented by -A-. Variances are weighted by sample size (N = 17, N = 18).

the point at which var $\hat{y}(\mathbf{x})$ is maximized—and the resulting VDG graphically shows the improvement. Certainly any enhancement of the stability of prediction variance can be easily digested by the user. Incidentally, the user can focus on the improvement provided by the augmentation in terms of G-efficiency. A G-optimal design has max N var $\hat{y}(\mathbf{x})/\sigma^2 = 5$. The design before augmentation gives max N var $\hat{y}(\mathbf{x})/\sigma^2 = 22.5$ (22.2% efficiency), and the value is reduced to approximately 12.6 (39.7% efficiency) after augmentation.

2.5 Properties of the VDG for the First-Order RSM Model

For the case 1 situation, there are interesting yet predictable properties that are apparent for V^r and R of $V(r)$. From Equation (2.4) it is apparent that the rate of change of V^r with respect to r is positive and increases as r increases. Thus *the average precision with which one estimates the response diminishes as one predicts further from the center*. This also is true for case 2, as one can readily observe by the development of V^r in Appendix B.

From Equations (2.5) and (2.6), we observe for case 1 that both the maximum and minimum of the variance function are increasing functions of r. When the design is not optimal in a variance sense [equal eigenvalues of $(X'X)^{-1}$], however, the max N var $\hat{y}(\mathbf{x})/\sigma^2$ increases faster than min N var $\hat{y}(\mathbf{x})/\sigma^2$, with the rate of change of R of $V(r)$ being given by

$$\frac{\partial\ R \text{ of } V(r)}{\partial r} = 2Nr(\lambda_{\max} - \lambda_{\min}).$$

Thus as one might expect, *the increase in instability in prediction variance on spheres* (as quantified by the range) *is greater for designs with a large spectrum in eigenvalues of* $(X'X)^{-1}$.

3. SECOND-ORDER DESIGNS—ILLUSTRATIONS

In this section, illustrations of the use of variance dispersion graphs are given for second-order response surface designs. We will use example displays to illustrate how the user can easily answer very pragmatic questions that deal with the performance of both standard and nonstandard designs.

The general expression for V^r given in Equation (2.2) applies for the second-order case. As a result, the V^r plot is certainly accessible for any second-order design. For the illustration of the range in the variance function, the function N var $\hat{y}(\mathbf{x})/\sigma^2$ was maximized and minimized over locations on the surface of a hypersphere. For the illustrations presented here, the computation was accomplished with a FORTRAN-based computing algorithm that computes the maximum and minimum of the variance function on a sphere. The algorithm, available on request (Vining 1988), also provides coordinates describing the location at which the maximum and minimum occur. This algorithm is adaptable to both first-order and second-order designs.

The search algorithm currently has the capability for handling designs through $k = 7$ variables. VDG's for three- or four-variable designs for a second-order model take roughly five seconds of central processing unit (CPU) time using an IBM 3084 processor complex. Evaluation of a five-variable design requires approximately one minute. A seven-variable case requires roughly five minutes of CPU time. In many situations, multiple locations exist for the maximum value of the variance on a particular sphere. As in the case of many optimization routines in which one has nonlinear equality constraints and the objective function is this complex, there is no guarantee of finding the global optimum. The regions exploited by the algorithm are spherical and cuboidal.

In Section 3.1, we use the VDG to compare various competing RSM designs. We also illustrate how the graphical procedure can be used to assess the impact of missing design points and answer other questions that often occur when one plans response surface experiments.

3.1 Hybrid and Small Composite Designs

A useful class of economical second-order RSM designs are the *small composite designs* (SCD) (see Draper 1982; Hartley 1959; Westlake 1965). Lucas (1976) provided an efficiency comparison of the small composite with other designs. The design consists of a Resolution III fraction of a 2^k factorial along with star or axial points and center runs. The resulting design is either saturated or near-saturated. Reasonable competition for the SCD is the class of *hybrid designs* developed by Roquemore (1976). The hybrid designs are also economical and represent a central composite type array for $k - 1$ variables with the levels of the kth variable selected to create certain design symmetries. The hybrid designs used in this illustration are the hybrid 310 and 311B developed by Roquemore. In each case, $k = 3$ and the design contains one center run. Both designs contain 11 runs. We have included one center run in the 310. The 311B, as originally developed by Roquemore, already contained a center run. The axial or star level on the SCD is $\alpha = 1.732$. All three designs are scaled so that the design perimeter is at radius $\sqrt{3}$. Khuri (1988) and Draper and Guttman (1988) discussed the hybrid in studies of measures of deviation from rotatability. Both hybrid designs and the SCD are shown in Table 1. Let us initially consider Figure 6,

Table 1. Design Matrices for the Hybrid 310 and 311B Designs and for a Small Composite Design With $\alpha = 1.732$

310			311B			SCD		
0	0	1.2906	0	0	$\sqrt{6}$	1	1	1
0	0	−.1360	0	0	$-\sqrt{6}$	1	−1	−1
−1	−1	.6386	−.7507	2.1063	1	−1	1	−1
1	−1	.6386	2.1063	.7507	1	−1	−1	1
−1	1	.6386	.7507	−2.1063	1	1.732	0	0
1	1	.6386	−2.1063	−.7507	1	−1.732	0	0
1.1736	0	−.9273	.7507	2.1063	−1	0	1.732	0
−1.1736	0	−.9273	2.1063	−.7507	−1	0	−1.732	0
0	1.1736	−.9273	−.7507	−2.1063	−1	0	0	1.732
0	−1.1736	−.9273	−2.1063	.7505	−1	0	0	−1.732
0	0	0	0	0	0	0	0	0

NOTE: For the illustration of Section 3.1, the design matrices have been scaled to have the furthest design point on a radius of $\sqrt{3} = 1.732$.

which shows the plot of V^r, the average N var $\hat{y}(\mathbf{x})/\sigma^2$ for the three designs. This interesting comparison reveals that both hybrid designs perform better, on the average, than the SCD. The graphical procedure also points out that the hybrid 310 design is considerably better than both competitors inside a radius of approximately 1.2. Near the design perimeter, however, the 311B has smaller values of the spherical variances.

Figure 7 shows the VDG reflecting the maximum and minimum of N var $\hat{y}(\mathbf{x})/\sigma^2$ around V^r for the SCD and the hybrid 310. (Note that we have now dropped the V^r symbol on the graph.) Figure 8 gives the same graph for the hybrid 311B and hybrid 310. None of the three designs show dispersion near the design center. The SCD, however, shows serious dispersion as one moves beyond radius 1.0. By contrast, both hybrids display more stability. The overall performance of the hybrid 310 is superior to that of the 311B until one nears the design perimeter. The prediction capability of the 310 is obviously inferior to the 311B beyond a radius of 1.2. The G-efficiency for the 311B is 91% as opposed to 45% for the 310. It is interesting here that the 311B clearly has a considerably higher G-efficiency, but this criterion does not reflect the superiority of the 310 in the design interior. The G-efficiencies of the two hybrid designs as depicted in the figure agree with values given by Roquemore.

3.2 Central Composite Design and Box–Behnken Design

The central composite and Box–Behnken designs are natural competitors as second-order RSM designs. Here we graphically compare the performance

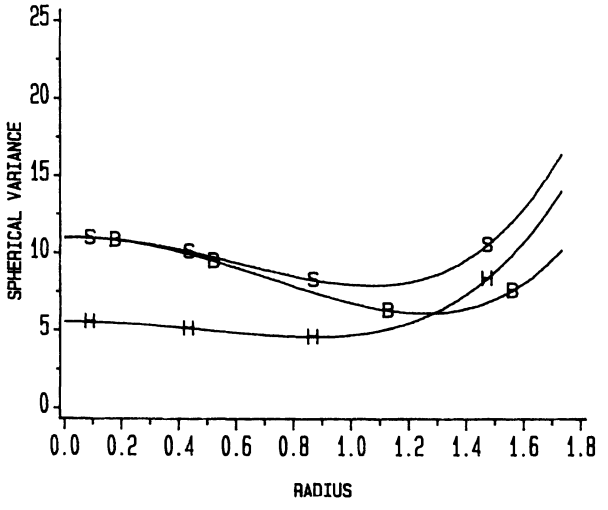

Figure 6. Comparison of Spherical Variances for an SCD and Hybrid 310 and 311B Designs. Design S is an SCD with $\alpha = 1.732$, $N = 11$, and one center run; design H is a hybrid 310 design with $N = 11$ and one center run; and design B is a hybrid 311B design with $N = 11$ and one center run. Variances are weighted by sample size.

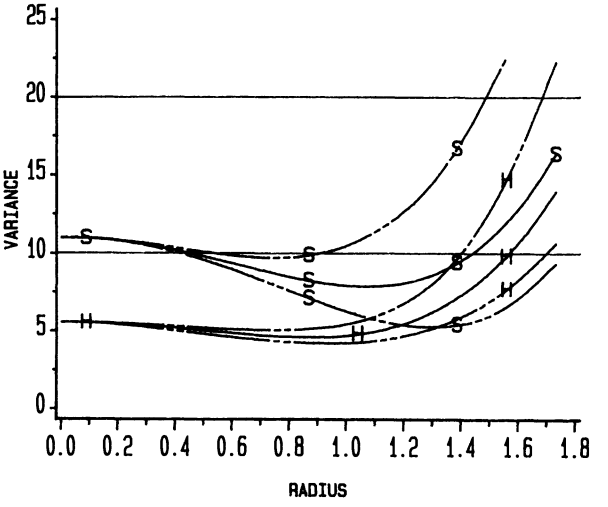

Figure 7. Variance Dispersion Graphs for an SCD and a Hybrid 310 Design. Design S is an SCD with $\alpha = 1.732$, $N = 11$, and one center run; design H is a hybrid 310 design with $N = 11$ and one center run. Variances are weighted by sample size.

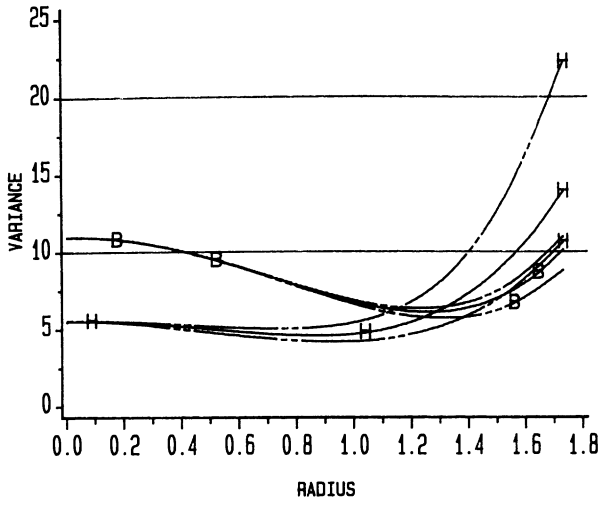

Figure 8. Variance Dispersion Graphs for a Hybrid 310 Design and a Hybrid 311B Design. Design H is a hybrid 310 design with N = 11 and one center run; design B is a hybrid 311B design with N = 11 and one center run. Variances are weighted by sample size.

of the central composite with axial parameter α = 1.0 and α = 1.682 and the Box–Behnken design. All three are k = 3 designs containing four center runs for this illustration. Figure 9 displays the spherical variances. Each design has been scaled so that the points on the design perimeter are at a distance $\sqrt{3}$. The α = 1.682 design is the rotatable central composite design (CCD). It is clear that, on the average, the performances of the rotatable CCD and the Box–Behnken design are nearly identical. As expected, the α = 1.0 central composite predicts best

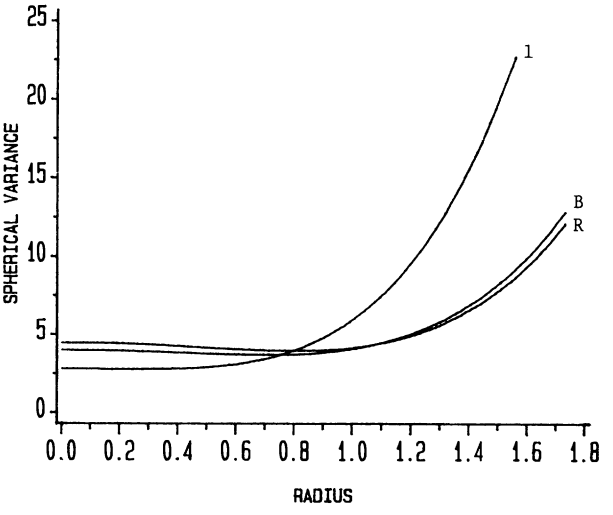

Figure 9. Comparison of Spherical Variances for Two CCD's and a Box–Behnken Design. Design R is a rotatable CCD with α = 1.682, N = 18, and four center runs; design 1 is a CCD with α = 1.0, N = 18, and four center runs; and design B is a Box–Behnken design with N = 16 and four center runs. Variances are weighted by sample size.

near the design center. To complete the comparison, Figures 10 and 11 display the dispersion around V^r for the Box–Behnken design and the α = 1.0 CCD. Again, all variances are weighted by sample size. Of course, the rotatable α = 1.682 CCD will have zero dispersion around V^r. The stability of the Box–Behnken design around V^r is quite good. On the other hand, the R of $V(r)$ is quite large for the CCD with α = 1.0, particularly beyond a radius of 1.0. This is certainly expected, since there is less information beyond radius 1.0 than in the case of the other two designs. This underscores the notion that a CCD with α = 1.0 should be used when the region of interest is strictly cuboidal rather than spherical. The design should not be used for predicting response outside the cube that describes the design. To make a more reasonable assessment of the α = 1.0 CCD, we offer Figure 12, in which the max N var $\hat{y}(\mathbf{x})/\sigma^2$ and min N var $\hat{y}(\mathbf{x})/\sigma^2$ were computed with the additional restriction that for any radius exceeding 1.0 the locations of the variances are restricted to being inside a unit cube. This picture best describes the performance of the design when prediction is restricted to the cube. Here the design performance is much better than that reflected in Figure 11.

3.3 Loss of Data Points: The Central Composite Design

Our next illustration of the VDG deals with an analysis of the impact of missing design points in an RSM design. The object of our illustration is a three-variable rotatable CCD (α = 1.682) with two star points missing—namely, (−1.682, 0, 0) and (0, 0, 1.682). Three center runs are used in the resulting

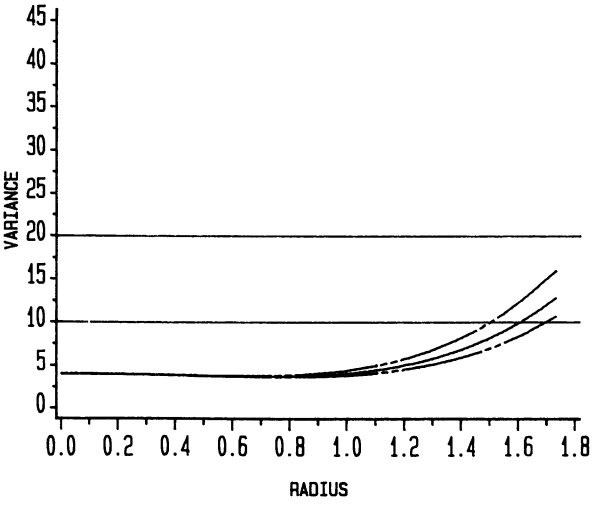

Figure 10. Variance Dispersion Graph for a Box–Behnken Design With N = 16 and Four Center Runs. Variances are weighted by sample size.

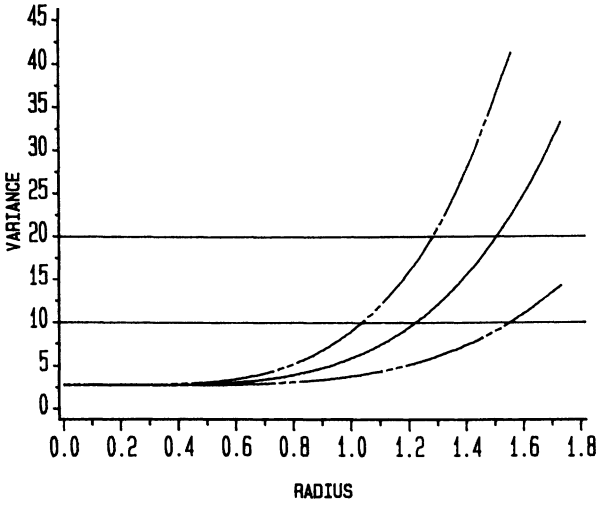

Figure 11. Variance Dispersion Graph for a CCD With α = 1.0, N = 18, and Four Center Runs. Variances are weighted by sample size.

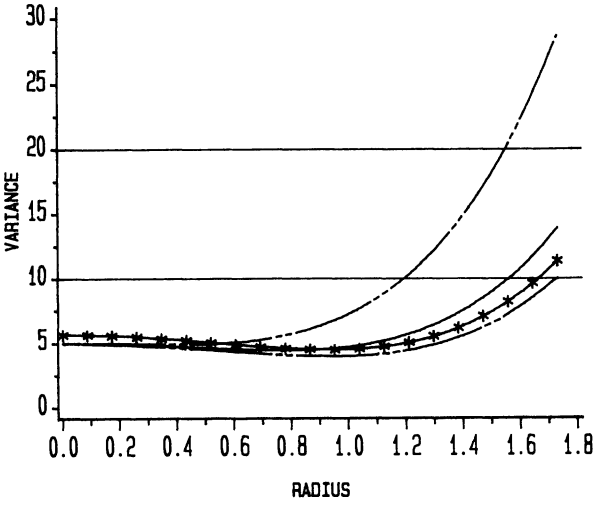

Figure 13. Variance Dispersion Graph for a CCD With Two Star Points Missing, α = 1.682, N = 15, and Three Center Runs. Spherical variances for the complete CCD (N = 17) are denoted by --. Variances are weighted by sample size.*

design. Figure 13 shows the VDG for the incomplete design and the V^r for the complete design. It is interesting that for predicting responses within a radius of about .7 the loss of the data points has little impact on quality. (The apparent advantage of the incomplete design is a result of weighting with sample size.) It is obvious that the deterioration in average performance is fairly modest. Nevertheless, the plot shows considerable instability as one moves away from the design center. The dispersion (as quantified by the range in variance) reveals how fragile the prediction has become due to the loss of information. This suggests that the loss of information does not result in uniform damage. This type of plot can provide the user with a simple picture that reveals the extent of the problem with missing data.

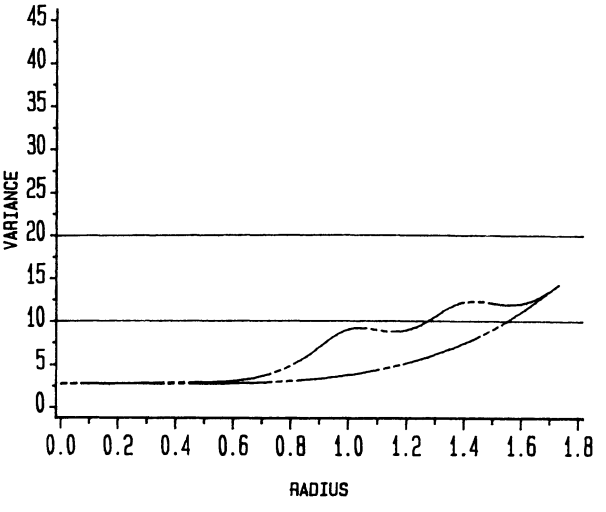

Figure 12. Maximum and Minimum Prediction Variances for a CCD With α = 1.0, N = 18, and Four Center Runs. Locations of the variances are restricted to be on or within the unit cube. Variances are weighted by sample size.

4. SUMMARY

It is important to point out that the illustrations given here are only illustrations and not definitive studies. The VDG approach has potential in the area of regions other than spherical and cuboidal—for example, the simplex region in the case of mixture designs. Exhaustive case studies involving standard RSM designs are difficult to report without displaying at least a few graphs. Conclusions found in comparisons between classes of designs depend sharply on values of design parameters, including the number of center runs. This is particularly true when one deals with rotatable or near-rotatable designs. It is our experience that the VDG for classes of saturated or near-saturated designs changes dramatically with a single augmentation. Moreover, what is a good picture for one user may not be attractive for another because of a priori knowledge concerning where in the design space one anticipates the need to explore.

Based on observations drawn up to this point, we offer the following:

1. For spherical regions, the rotatable CCD and the Box–Behnken design compare very favorably. The CCD, as expected, benefits greatly from two or three center runs, but the Box–Behnken design certainly should contain two center runs to achieve an attractive variance picture.

2. Using α considerably smaller than the rotatable value for the CCD results in poor prediction per-

formance close to the design perimeter in the case of a spherical region. For example, for $k = 3$ with α as small as 1.35, the maximum value of $N \operatorname{var} \hat{y}(\mathbf{x})/\sigma^2$ increases by as much as 40% above that of the rotatable design or the equiradial design. The advantage experienced at the design center with the use of a smaller α is minimal when the design contains at least three center runs.

3. Roquemore's hybrid designs appear to be very promising; this includes the six-variable 628A, which is not discussed here. They are all very near rotatable (or exactly rotatable) and are generally benefited greatly by augmentation with one or two extra center runs.

There is considerable potential in the area of design augmentation—that is, determining graphically the nature of the gain produced by augmenting a design. In addition to a graphical depiction of design capability, the VDG graphically allows for a sequential (interactive) generation of D-optimal designs. There is considerable interest in the benefit of replicating at locations other than the design center. This approach can be used to assess the advantage of replicating axial points, for example, rather than center points.

Interesting information regarding robustness of RSM designs to errors in controlling design levels can easily be retrieved. One merely displays the VDG of the design in question and compares with the "ideal"—that is, the "target" design. The approach discussed here can be adapted to accommodate situations involving anticipated outliers, failure of homogeneous variance assumptions, other forms of estimation, and so forth. Studies of the impact of center runs and replication at other design locations are easily undertaken.

Some attention has focused lately on measuring *nearness to rotatability* of a design (see Draper and Guttman 1988; Khuri 1988). The R of $V(r)$ measures dispersion on spheres, depicting deviation from rotatability. For example, this notion is nicely illustrated in the graphics displayed in the Box–Behnken and the hybrid designs. Clearly the hybrid 311B and the $k = 3$ Box–Behnken designs are very close to being rotatable according to the relatively small R of V displayed in the pictures.

Variance dispersion graphs allow the user of an experimental design to view a "footprint" that describes the performance throughout a region in which responses are to be estimated. The analyst can determine, for example, the severity of the deterioration of prediction capability close to the design or region perimeter. Comparison among competing designs can be made easily, and strengths and weaknesses can be assessed; this type of information cannot be captured in *single efficiency numbers*.

A catalog of VDG's for commonly used response surface designs has been prepared (see Myers, Giovannitti-Jensen, and Vining 1989). This catalog shows the effect of design parameters and provides the user an aid in choosing a design.

APPENDIX A: SPHERICAL REGION MOMENTS

A.1 Spherical Region Moments Through Order 4

Spherical region moments are used in the development of model-specific forms for the spherical variance and for the variance of $N \operatorname{var}(\hat{y}(\mathbf{x}))/\sigma^2$ for locations on the surface of a hypersphere defined by $U_r = \{\mathbf{x} : \sum_{i=1}^{k} x_i^2 = r^2\}$. A spherical region moment of order δ is defined to be

$$\sigma_{\delta_1\delta_2\cdots\delta_k} = \Psi \int_{U_r} x_1^{\delta_1} x_2^{\delta_2} \cdots x_k^{\delta_k} \, d\mathbf{x},$$

where $\Psi^{-1} = \int_{U_r} d\mathbf{x}$ is the surface area of U_r and $\sum_{i=1}^{k} \delta_i = \delta$. Since U_r is a symmetric region, the spherical moment $\sigma_{\delta_1\delta_2\cdots\delta_k}$ is 0 whenever any δ_i is odd.

The spherical region moments that are used in the development of the spherical variance for the first-order and second-order model cases are the second-order and fourth-order spherical moments given by

$$\sigma_2 = \Psi \int_{U_r} x_i^2 \, d\mathbf{x} = \frac{r^2}{k},$$

$$\sigma_4 = \Psi \int_{U_r} x_i^4 \, d\mathbf{x} = \frac{3r^4}{k(k+2)},$$

$$\sigma_{22} = \Psi \int_{U_r} x_i^2 x_j^2 \, d\mathbf{x} = \frac{r^4}{k(k+2)}.$$

A.2 The Spherical Region Moment Matrix for First-Order and Second-Order Models in Three Variables

To illustrate the form of the spherical region moment matrix S in the definition of V^r [Eq. (2.2)] consider a first-order model in $k = 3$ variables. In this case, evaluation of (2.3) gives

$$S = \begin{bmatrix} 1 & 0 & 0 & 0 \\ 0 & \sigma_2 & 0 & 0 \\ 0 & 0 & \sigma_2 & 0 \\ 0 & 0 & 0 & \sigma_2 \end{bmatrix}$$

with σ_2, the second-order spherical moment, defined in Section A.1.

For a second-order model in $k = 3$ variables, the

matrix of spherical region moments is

$S =$

	x_1	x_2	x_3	x_1^2	x_2^2	x_3^2	x_1x_2	x_1x_3	x_2x_3
	1	0	0	0	σ_2	σ_2	σ_2	0	0	0
x_1	0	σ_2	0	0	0	0	0	0	0	0
x_2	0	0	σ_2	0	0	0	0	0	0	0
x_3	0	0	0	σ_2	0	0	0	0	0	0
x_1^2	σ_2	0	0	0	σ_4	σ_{22}	σ_{22}	0	0	0
x_2^2	σ_2	0	0	0	σ_{22}	σ_4	σ_{22}	0	0	0
x_3^2	σ_2	0	0	0	σ_{22}	σ_{22}	σ_4	0	0	0
x_1x_2	0	0	0	0	0	0	0	σ_{22}	0	0
x_1x_3	0	0	0	0	0	0	0	0	σ_{22}	0
x_2x_3	0	0	0	0	0	0	0	0	0	σ_{22}

with σ_2, σ_4, and σ_{22} as defined in Section A.1.

APPENDIX B: DEVELOPMENT OF THE VDG FOR THE FIRST-ORDER MODEL

B.1 Development of the Spherical Variance Under Case 1

Suppose a first-order model in k variables is fit to the response with a design centered about the center of the region of interest (case 1). Let $\mathbf{x} = (x_1x_2 \cdots x_k)'$ be a setting of the levels of the variables $x_1, x_2, \ldots, x_k$. Partition the $N \times (k + 1)$ model matrix X by $[\mathbf{1} \quad X^*]$ where $\mathbf{1}$ is an $N \times 1$ vector of ones and X^* is the $N \times k$ design matrix. The first-order model can be written as $E(\mathbf{y}) = X\boldsymbol{\beta}$, where $\boldsymbol{\beta} = (\beta_0\beta_1 \cdots \beta_k)'$ is the vector of regression coefficients of the first-order model.

In the present discussion, the columns of the submatrix X^* are centered so that $\sum_{i=1}^N x_{ij} = 0$ for all $j = 1, 2, \ldots, k$. In this way, the vector of ones in X is orthogonal to the submatrix X^*. Thus

$$(X'X)^{-1} = \begin{bmatrix} 1/N & \mathbf{0}' \\ \mathbf{0} & (X^{*\prime}X^*)^{-1} \end{bmatrix}.$$

Consider the eigenvalue decomposition of $(X^{*\prime}X^*)^{-1}$. Define P to be the $k \times k$ orthogonal matrix for which $P'(X^{*\prime}X^*)^{-1}P = \Lambda$, where $\Lambda = \text{diag}(\lambda_1, \lambda_2, \ldots, \lambda_k)$ is the diagonal matrix containing the eigenvalues of $(X^{*\prime}X^*)^{-1}$. The variance of a predicted response for case 1 can be written as

$$\text{var}(\hat{y}(\mathbf{x})) = \sigma^2 \left[\frac{1}{N} + \mathbf{x}'PP'(X^{*\prime}X^*)^{-1}PP'\mathbf{x}\right]$$

$$= \sigma^2 \left[\frac{1}{N} + \sum_{i=1}^k \lambda_i z_i^2\right], \qquad \text{(B.1)}$$

where $\mathbf{z} = (z_1z_2 \cdots z_k)' = P'\mathbf{x}$. Note that $\sum_{i=1}^k z_i^2 = \mathbf{z}'\mathbf{z} = \mathbf{x}'\mathbf{x} = \sum_{i=1}^k x_i^2$. Thus, for any point $\mathbf{x}$ located on U_r, $\mathbf{z} = P'\mathbf{x}$ is also on U_r.

Under case 1 then, the average of the variances of the estimated responses over the surface of the k-dimensional hypersphere defined by U_r, the spherical variance given by (2.1), is

$$V^r = \Psi \int_{U_r} \left(1 + N \sum_{i=1}^k \lambda_i z_i^2\right) d\mathbf{z}$$

$$= 1 + N\frac{r^2}{k}\sum_{i=1}^k \lambda_i.$$

B.2 The Maximum and Minimum Prediction Variance On a Sphere Under Case 1

To find a specific form for the R of V under the specifications of case 1, it is necessary to find the optimum values for $N \text{ var}(\hat{y}(\mathbf{x}))/\sigma^2$ when $\mathbf{x}$ is in U_r. From Section B.1, $\text{var}(\hat{y}(\mathbf{x}))/\sigma^2$ is given by Equation (B.1) under case 1. The coefficients, $\lambda_1, \ldots, \lambda_k$, of the variables in the function are the eigenvalues of the full rank matrix $(X^{*\prime}X^*)^{-1}$ and hence positive. For convenience, suppose that the variables are ordered in such a way that $0 < \lambda_{\min} = \lambda_1 \leq \lambda_2 \leq \cdots \leq \lambda_k = \lambda_{\max}$.

First consider the case in which the eigenvalues are all distinct; that is, $0 < \lambda_1 < \lambda_2 < \cdots < \lambda_k$. To maximize (B.1) subject to the condition that $\sum_{i=1}^k x_i^2 = \sum_{i=1}^k z_i^2 = r^2$ requires that the variable whose coefficient is the largest—that is, the variable that has the highest weight—be as large as possible. Thus, for the first-order case, the maximum variance of prediction on U_r occurs for $z_k = \pm r$ and $z_1 = z_2 = \cdots = z_{k-1} = 0$ to achieve $\sum_{i=1}^k z_i^2 = r^2$. The corresponding maximum is

$$\max_{\mathbf{x}\in U_r} \frac{N}{\sigma^2} \text{var}(\hat{y}(\mathbf{x}))$$

$$= \max_{\mathbf{z}\in U_r} \left[1 + N \sum_{i=1}^k \lambda_i z_i^2\right] = 1 + N\lambda_{\max}r^2,$$

where $\lambda_{\max}$ is the largest eigenvalue of $(X^{*\prime}X^*)^{-1}$.

In a similar fashion, we can show that

$$\min_{\mathbf{x}\in U_r} \frac{N}{\sigma^2} \text{var}(\hat{y}(\mathbf{x}))$$

$$= \min_{\mathbf{z}\in U_r} \left[1 + N \sum_{i=1}^k \lambda_i z_i^2\right] = 1 + N\lambda_{\min}r^2,$$

where $\lambda_{\min}$ is the smallest eigenvalue of $(X^{*\prime}X^*)^{-1}$.

When two or more of the eigenvalues are the same, the maximum and minimum values may occur at more than one point on U_r. The resulting optimal values, however, remain the same. As an illustration, consider $\lambda_{\min} = \lambda_1 = \lambda_2$ and all other eigenvalues distinct. Clearly, the maximum prediction variance at locations on U_r is as before. The minimum, however, may occur at any point on U_r for which $z_1^2 + z_2^2 = r^2$ and, hence, $z_3 = \cdots = z_k = 0$. The corresponding minimum value though is $1 + N\lambda_{\min}r^2$,

where $\lambda_{\min} = \lambda_1 = \lambda_2$ is the smallest eigenvalue of $(X^{*\prime}X^*)^{-1}$. So the optimum values of the prediction variance on U_r are not effected by multiplicities in the eigenvalues of $(X^{*\prime}X^*)^{-1}$.

B.3 Development of the Spherical Variance Under Case 2

Let us define the location of the center of the design to be $\mathbf{h} = (h_1 h_2 \cdots h_k)'$; the center of the region is $\mathbf{0} = (0\,0 \cdots 0)'$ in the design variables. When $\mathbf{h} \neq \mathbf{0}$, the columns of the submatrix X^* are not centered. It will prove useful to consider a translation of the axis system corresponding to the design variables $x_1, x_2, \ldots, x_k$ to an axis system with origin at the center of the design. Call the variables in the new axis system $w_1, w_2, \ldots, w_k$, where $w_i = x_i - h_i$ and $i = 1, 2, \ldots, k$.

In terms of the w variables, the variance of a predicted response at a point $\mathbf{w} = (w_1 w_2 \cdots w_k)' = \mathbf{x} - \mathbf{h}$ is given by $\text{var}(\hat{y}(\mathbf{w})) = \sigma^2 \mathbf{f}'(\mathbf{w})(W'W)^{-1}\mathbf{f}(\mathbf{w})$, where $\mathbf{f}(\mathbf{w}) = (1\ \mathbf{w})'$ and $W = [1 \quad W^*]$. The $N \times k$ submatrix W^* is analogous to the submatrix X^* in case 1 (see Sec. B.1). In this case, the columns of W^* are centered versions of the corresponding columns of X^*. Using the development of case 1 for a prediction variance at a location in the w-axis system, $\text{var}(\hat{y}(\mathbf{w})) = \sigma^2[1/N + \mathbf{w}'(W^{*\prime}W^*)^{-1}\mathbf{w}]$.

It will be convenient to express the prediction variance in terms of the eigenvalues of the $(W^{*\prime}W')^{-1}$ matrix. Let P be the $k \times k$ orthogonal matrix of the eigenvalue decomposition of $(W^{*\prime}W^*)^{-1}$. Then

$$\begin{aligned}\text{var}(\hat{y}(\mathbf{w})) &= \sigma^2\left[\frac{1}{N} + \mathbf{z}'\Lambda\mathbf{z} - 2\mathbf{z}'\Lambda\mathbf{m} + \mathbf{m}'\Lambda\mathbf{m}\right] \\ &= \sigma^2\left[\frac{1}{N} + \sum_{i=1}^{k}\lambda_i z_i^2 - 2\sum_{i=1}^{k}\lambda_i m_i z_i + \sum_{i=1}^{k}\lambda_i m_i^2\right], \qquad \text{(B.2)}\end{aligned}$$

where $\mathbf{z} = (z_1 z_2 \cdots z_k)' = P'\mathbf{x}$ and $\mathbf{m} = (m_1 m_2 \cdots m_k)' = P'\mathbf{h}$. $\Lambda = \text{diag}(\lambda_1, \lambda_2, \ldots, \lambda_k)$ is the diagonal matrix containing the eigenvalues of $(W^{*\prime}W^*)^{-1}$. Note that if the design is centered about the origin of the region in the design variables—that is, if $\mathbf{h} = \mathbf{0}$—this formulation reduces, as it should, to the expression given in (B.1).

Consider the evaluation of V^r in the w-axis system. The prediction variances to be averaged in this case correspond to locations $\mathbf{w} = (w_1 w_2 \cdots w_k)'$ on the surface of the hypersphere of radius r with center at $\mathbf{w} = \mathbf{0} - \mathbf{h}$. Let $U_r^w = \{\mathbf{w} : \sum_{i=1}^{k}(w_i + h_i)^2 = r^2\}$ denote the surface of this hypersphere and $\Psi_w^{-1} = \int_{U_r^w} d\mathbf{w}$ be the surface area of U_r^w. Then,

$$\begin{aligned}V^r &= \frac{N\Psi_w}{\sigma^2}\int_{U_r^w}\text{var}(\hat{y}(\mathbf{w}))\,d\mathbf{w} \\ &= N\Psi\int_{U_r}\left(\frac{1}{N} + \sum_{i=1}^{k}\lambda_i z_i^2 - 2\sum_{i=1}^{k}\lambda_i m_i z_i + \sum_{i=1}^{k}\lambda_i m_i^2\right)d\mathbf{z} \\ &= 1 + N\frac{r^2}{k}\sum_{i=1}^{k}\lambda_i + N\sum_{i=1}^{k}\lambda_i m_i^2\end{aligned}$$

by a transformation of variables and (B.2). The interim steps required in this formulation appear in Giovannitti-Jensen (1987).

B.4 The R of V Under Case 2

When the center of the design is not the same as the center of the region, the problem of optimizing $N\,\text{var}(\hat{y}(\mathbf{x}))/\sigma^2$ subject to $\mathbf{x} = (x_1 x_2 \cdots x_k)'$ being on the surface of a hypersphere of radius r centered at $\mathbf{x} = \mathbf{0}$ is equivalent to the constrained optimization of $N\,\text{var}(\hat{y}(\mathbf{w}))/\sigma^2$ in the w variables. In terms of the w-axis system defined in Section B.3, the constraint requires that the point $\mathbf{w} = (w_1 w_2 \cdots w_k)'$ lie on the surface of a hypersphere of radius r with center at $\mathbf{w} = \mathbf{0} - \mathbf{h}$.

Using the method of Lagrangian multipliers for finding the stationary points of a function, the maximum and minimum values are found by solving the following set of simultaneous equations:

$$\frac{\partial Q}{\partial w_1} = 0, \frac{\partial Q}{\partial w_2} = 0, \quad \ldots \quad \frac{\partial Q}{\partial w_k} = 0, \frac{\partial Q}{\partial \mu} = 0,$$

where

$$\begin{aligned}Q &= \frac{N}{\sigma^2}\text{var}(\hat{y}(\mathbf{w})) - \mu\left[\sum_{i=1}^{k}(w_i + h_i)^2 - r^2\right] \\ &= 1 + N\mathbf{w}'(W^{*\prime}W^*)^{-1}\mathbf{w} - \mu[(\mathbf{w} + \mathbf{h})'(\mathbf{w} + \mathbf{h}) - r^2],\end{aligned}$$

and μ is the Lagrangian multiplier. The solution to this problem appears in Giovannitti-Jensen (1987).

[*Received March 1988. Revised November 1988.*]

REFERENCES

Atwood, C. L. (1969), "Optimal and Efficient Designs of Experiments," *The Annals of Mathematical Statistics*, 40, 1570–1602.

Box, G. E. P., and Behnken, D. W. (1960), "Some New Three-Level Designs for the Study of Quantitative Variables," *Technometrics*, 2, 455–475.

Box, G. E. P., and Draper, N. R. (1959), "A Basis for the Se-

lection of a Response Surface Design," *Journal of the American Statistical Association*, 54, 622–654.

——— (1963), "The Choice of a Second Order Rotatable Design," *Biometrika*, 50, 335–352.

——— (1987), *Empirical Model-Building and Response Surfaces*, New York: John Wiley.

Box, G. E. P., and Hunter, J. S. (1957), "Multifactor Experimental Designs for Exploring Response Surfaces," *The Annals of Mathematical Statistics*, 28, 195–241.

Box, G. E. P., and Wilson, K. B. (1951), "On the Experimental Attainment of Optimum Conditions," *Journal of the Royal Statistical Society*, Ser. B, 13, 1–45.

Box, M. J., and Draper, N. R. (1971), "Factorial Designs, the $|X'X|$ Criterion, and Some Related Matters," *Technometrics*, 13, 731–742.

——— (1974), "On Minimum-Point Second-Order Designs," *Technometrics*, 16, 613–616.

Draper, N. R. (1982), "Center Points in Second-Order Response Surface Designs," *Technometrics*, 24, 127–133.

Draper, N. R., and Guttman, I. (1988), "An Index of Rotatability," *Technometrics*, 30, 105–111.

Draper, N. R., and Lawrence, W. E. (1965), "Designs Which Minimize Model Inadequacies: Cuboidal Regions of Interest," *Biometrika*, 52, 111–118.

Giovannitti-Jensen, A. (1987), "Graphical Assessment of the Prediction Capability of Response Surface Designs," unpublished dissertation, Virginia Polytechnic Institute and State University, Dept. of Statistics.

Hartley, H. O. (1959), "Smallest Composite Designs for Quadratic Response Surfaces," *Biometrics*, 15, 611–624.

Hoerl, A. E. (1959), "Optimum Solution of Many Variables Equations," *Chemical Engineering Progress*, 55, 69–78.

Hoke, A. T. (1974), "Economical Second-Order Designs Based on Irregular Fractions of the 3^n Factorial," *Technometrics*, 16, 375–384.

Hussey, J. R., Myers, R. H., and Houck, E. C. (1987), "Correlated Simulation Experiments in First Order Response Surface Design," *Operations Research*, 35, 744–758.

Khuri, A. I. (1988), "A Measure of Rotatability for Response-Surface Designs," *Technometrics*, 30, 95–104.

Khuri, A. I., and Cornell, J. A. (1987), *Response Surfaces*, New York: Marcel Dekker.

Kiefer, J. (1959), "Optimum Experimental Designs" (with discussion), *Journal of the Royal Statistical Society*, 21, 272–319.

Lucas, J. M. (1974), "Optimum Composite Designs," *Technometrics*, 16, 561–567.

——— (1976), "Which Response Surface Design Is Best," *Technometrics*, 18, 411–417.

Mitchell, T. J. (1974), "An Algorithm for the Construction of *D*-Optimal Experimental Designs," *Technometrics*, 16, 203–210.

Mitchell, T. J., and Bayne, C. K. (1978), "*D*-Optimal Fractions of Three-Level Factorial Designs," *Technometrics*, 20, 369–380.

Myers, R. H. (1976), *Response Surface Methodology*, Blacksburg, VA: Author.

Myers, R. H., Giovannitti-Jensen, A., and Vining, G. (1989), "Variance Dispersion Graphs for Various Response Surface Designs: Spherical and Cuboidal Regions," Technical Report 89-1, Virginia Polytechnic Institute and State University, Dept. of Statistics.

Nalimov, V. V., Golikova, T. I., and Mikeshina, N. G. (1970), "On Practical Use of the Concept of *D*-Optimality," *Technometrics*, 12, 799–812.

Notz, W. (1982), "Minimal Point Second Order Designs," *Journal of Statistical Planning and Inference*, 6, 47–58.

Roquemore, K. G. (1976), "Hybrid Designs for Quadratic Response Surfaces," *Technometrics*, 18, 419–423.

St. John, R. C., and Draper, N. R. (1975), "*D*-Optimality for Regression Designs: A Review," *Technometrics*, 17, 15–23.

Stroud, A. H. (1971), *Approximate Calculation of Multiple Integrals*, Englewood Cliffs, NJ: Prentice-Hall.

Vining, G. (1988), "An Algorithm for Graphical Assessment of Experimental Designs," Technical Report 88-3, Virginia Polytechnic Institute and State University, Dept. of Statistics.

Westlake, W. J. (1965), "Composite Designs Based on Irregular Fractions of Factorials," *Biometrics*, 21, 324–336.